

# Wettability of Microstructured Hydrophobic Sol-Gel Coatings

S. PILOTEK\* AND H.K. SCHMIDT

*Institut für Neue Materialien, Saarbrücken, Deutschland*

pilotek@inm-gmbh.de

schmidt@inm-gmbh.de

**Abstract.** The formation of appropriate surface patterns on hydrophobic surfaces leads to a general change in their wettability and the contact angle increases substantially. Such coatings are of great technical interest, especially if aqueous media are concerned as in the prevention of ice-adhesion. For this reason various fluorine containing nanocomposite coatings have been developed by sol-gel processing.

The morphology of these hydrophobic surfaces has been controlled by varying the content of silica particles regarding size, degree of aggregation, and concentration. The wettability is characterized by the measurement of dynamic contact angles against water. The complete range of different wettability regimes is accessible, i.e. smooth surfaces (both low advancing contact angle and hysteresis between advancing and receding contact angle), surfaces within the Wenzel regime (high advancing contact angle and hysteresis), and superhydrophobic surfaces (high advancing contact angle and low hysteresis). The wettability is correlated with the surface roughness as determined using a profilometer or AFM.

The wettability of superhydrophobic surfaces is greatly dependent on the surface tension of the liquid. By comparison of the tiltangle  $\theta_t$  of a smooth and a superhydrophobic surface, a critical surface tension  $\gamma_c$  is identified, where  $\theta_t$  (smooth surface) =  $\theta_t$  (microstructured surface). The microstructured surface provides a better run-off of liquids  $\gamma_{lg} > \gamma_c \approx 55 \text{ mN} \cdot \text{m}^{-1}$ .

**Keywords:** hydrophobic, coating, roughness, super-water repellent, superhydrophobic

## Introduction

Nanomer<sup>®</sup> is a versatile materials technology developed by INM comprising inorganic-organic hybrid networks and nanoparticles based on the Sol-Gel-process [1]. Especially useful are nanomers that contain fluoroalkyl components which can be used as hydrophobic coatings. The fluoroalkyl containing components are surface-active and are therefore concentrated at the liquid (lacquer)—gas (air) interface. In contrast, only a small concentration of these components is present at the solid (substrate)—liquid (lacquer) interface such that a good adhesion on various substrates is feasible. After curing the antiadhesive properties of smooth antiadhesive nanomer coatings are comparable to those

of perfluorinated organic polymers (contact angle vs. water  $107^\circ$ , contact angle vs. hexadecane  $50^\circ$ ) [2].

Microstructured surfaces faced considerable attention in recent years and some systems have been further developed, e.g. surfaces based on porous aluminum-oxide [3]. Here we present investigations concerning the wettability of nanoparticle-structured antiadhesive nanomer coatings.

## Theory

An early theoretical description of the influence of morphology on wettability was given by Wenzel (Eq. (1)), who assumed a linear dependence of  $\cos \theta_{\text{obs}}$  from  $\cos \theta_0$ , the intrinsic contact angle (c.a.) of an ideal surface of the respective material given by the well-known Young equation. The slope  $r_W$  of the linear equation is

\*To whom all correspondence should be addressed.

given as the roughness of the surface and expressed as the ratio of real to nominal area of the surface.

$$\cos \theta_{\text{obs}} = r_w \cos \theta_0 \quad (1)$$

Cassie and Baxter investigated hydrophobic textiles where a drop of water cannot rest solely on the solid but has also contact to air at the substrate-side of the drop. Their equation expresses this idea by reflecting the area where a liquid is in contact with the material ( $Q_1$  with c.a.  $\theta_0$ ) and where the liquid is in contact with air ( $Q_2$  with c.a.  $\theta_{\text{air}} = 180^\circ$ ), normalized to the nominal area, respectively. The same idea applies to extremely porous hydrophobic substrates, where air is enclosed between liquid and substrate.

$$\cos \theta_{\text{obs}} = Q_1 \cos \theta_0 - Q_2 \quad (2)$$

Johnson and Dettre showed that there is a scope of application for both models.[3] At small roughnesses, the Wenzel-Regime is identified whereas at extreme roughnesses superhydrophobic surfaces are observed, where the model of Cassie and Baxter is applicable. Water possesses a remarkably high mobility on the latter. Because this is a dynamic phenomenon, wettability of structured surfaces should be discussed in terms of dynamic c.a. rather than the static. Johnson and Dettre point out that surfaces of the Wenzel-Regime should have increased static (and advancing) c.a. but low receding contact angles resulting in high hysteresis between advancing and receding c.a. For superhydrophobic surfaces both high advancing and receding c.a. are expected and therefore a small hysteresis. McCarthy et al. also stress the importance of hysteresis in discussing the wettability of rough hydrophobic surfaces [4]. They point out that morphology itself has an impact on wettability. Superhydrophobic surfaces should be more eas-

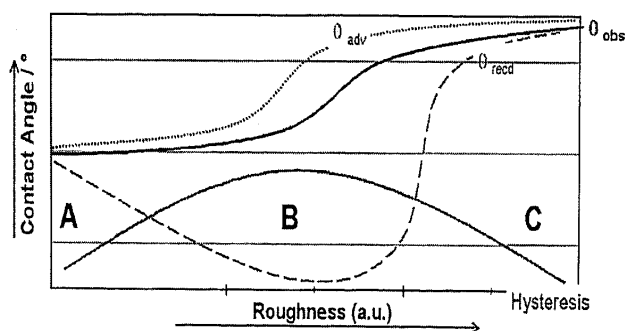


Figure 1. Wettability vs. roughness (schematically). (A) Smooth surface, (B) Wenzel Regime, (C) superhydrophobic surface.  $\theta_{\text{obs}}$ : observable (static) c.a.,  $\theta_{\text{adv}}$ : advancing c.a.,  $\theta_{\text{recd}}$ : receding c.a.

ily obtained on random structures than on regular patterns, because here the three phase (solid-liquid-gas) contact line is more easily destabilized. Figure 1 summarizes the dependencies of wettability on roughness as expected from theory.

## Experimental Section

A sol is made by hydrolysis and condensation of 9.61 g (46.1 mmol) tetraethoxysilane, 2.31 g (4.5 mmol) 1H, 1H,2H,2H-perfluorooctyltriethoxysilane and 1.85 ml (103 mmol) 0.1 N aqueous HCl in iso-propanol.

*Series I:* Different types of silica are dispersed into the sol, such that the additional silica content of the cured coatings is 70 vol%. Monodispersed particles (diameter 10 nm [P1] and 100 nm [P2]) and fumed silica (primary diameter 15 nm [P3]) are employed. The material is applied to glass substrates by spin coating and cured at 150°C for 1 h.

*Series II:* Various amounts of fumed silica is given to the sol, such that the additional silica content of the cured coatings is 0–45 wt%. The material is applied to glass substrates by spin coating and cured at 150°C for 1 h.

Opaque coatings are obtained where fumed silica is employed.

The roughness is determined using a Collotec Nanosurf 500 profilometer or an AFM.

The dynamic c.a. are determined by variation of the drop volume on a Krüss GII.

The tiltangle is determined using an apparatus, that tilts a substrate with a drop of liquid until the drop moves. The apparatus stops and the respective angle can be read. Liquids of different surface tension are made by appropriate mixtures of acetone and water. The surface tension of each mixture is determined using a tensiometer (Krüss, plate geometry). The mixtures are carefully sealed until measurement. A possible change in surface tension during the measurement is neglected.

## Results

In series I of the experiments the influence of a high content of different silica particles in the basis material is investigated. The coatings are characterized by REM, profilometer and wettability against water. Visually, the matrix without particles as well as sample P1 (containing 10 nm particles) are transparent, whereas P2 and P3 have an opaque appearance.

Table 1. Particle diameter  $d$  of employed silica and surface roughness  $R_a$  of sol-gel coatings.

Sample	$d/\text{nm}$	$R_a/\text{nm}$
Matrix	—	15
P1	10	30
P2	100	136
P3	Fumed, 15	3282

REM measurements of the coatings are undertaken to characterize the morphology. They confirm that the morphology of the coatings is dominated by the respective silica particles, where employed. Especially P3 exhibits a random structure. Surface roughness determinations as well reflect the particles used (Table 1). The surface roughness is increased drastically from the matrix (M) to P3. Figure 2 illustrates the wettability of the different coatings.

All of the coatings are hydrophobic as shown by their high advancing c.a. ( $>90^\circ$ ). Identifying that roughness increases drastically from M to P3, the differences in wettability reflect the theoretically expected dependence on roughness. M is a typical smooth, hydrophobic surface and P3 is superhydrophobic with a hysteresis  $<10^\circ$ , whereas P1 and P2 are best characterized as surfaces of the Wenzel-Regime. Therefore, the complete range of different wettability regimes is accessible by this technique.

Series II of experiments addresses the influence of silica concentration in the coatings. Increasing the content of fumed silica should result in a variation of surface roughness as in series I. Unexpectedly, the mean rough-

ness  $R_a$  does not correlate with a silica content between 0–45%. Instead,  $R_a$  rises to a critical range (30–70 nm, Fig. 3) and remains about constant. So a difference in roughness between coatings containing 20, 30 or 45% silica is not detectable. The wettability of these different randomly microstructured coatings is illustrated in Fig. 4.

The wettability of the surfaces of series II varies greatly with silica content. All of the coatings are hydrophobic and the samples span the complete range of wettability regimes. A coating with 45% silica is superhydrophobic with a hysteresis of  $<1^\circ$ , thus higher concentrations were not considered. It is interesting to note that the investigated surfaces reflect the theoretically expected dependence on roughness, though an increase

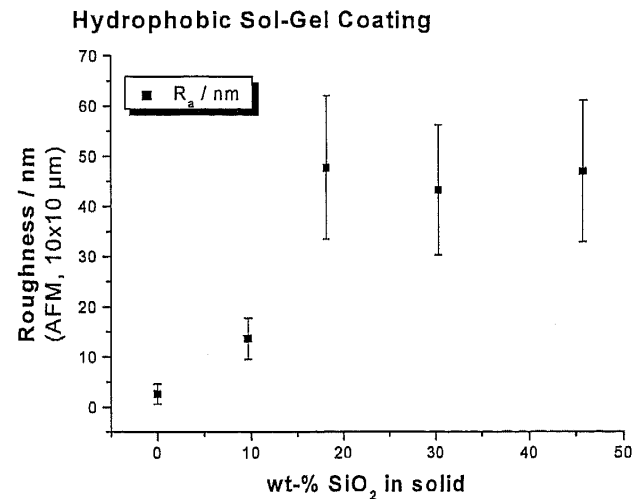


Figure 3. Mean roughness ( $R_a$ ) of microstructured, hydrophobic sol-gel coatings vs. silica content.

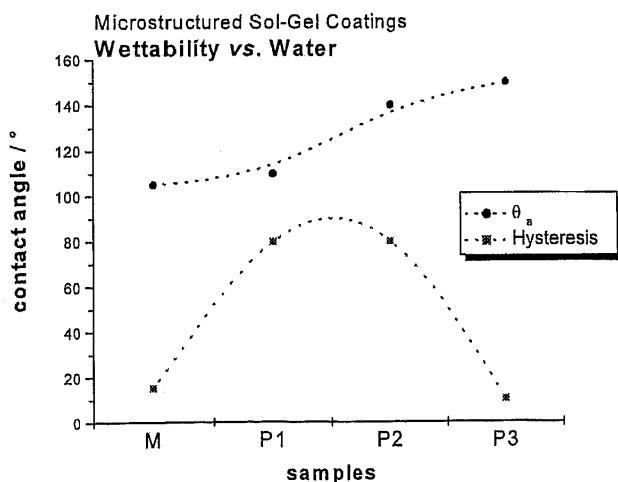


Figure 2. Dynamic wettability of different microstructured, hydrophobic sol-gel coatings.

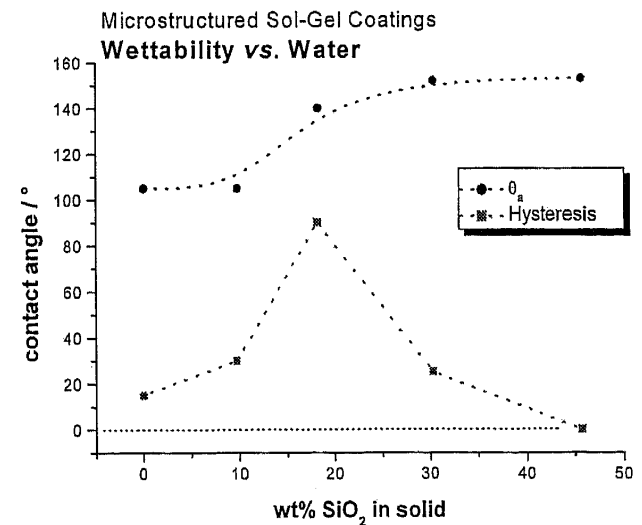


Figure 4. Dynamic wettability of microstructured, hydrophobic sol-gel coatings vs. silica content.

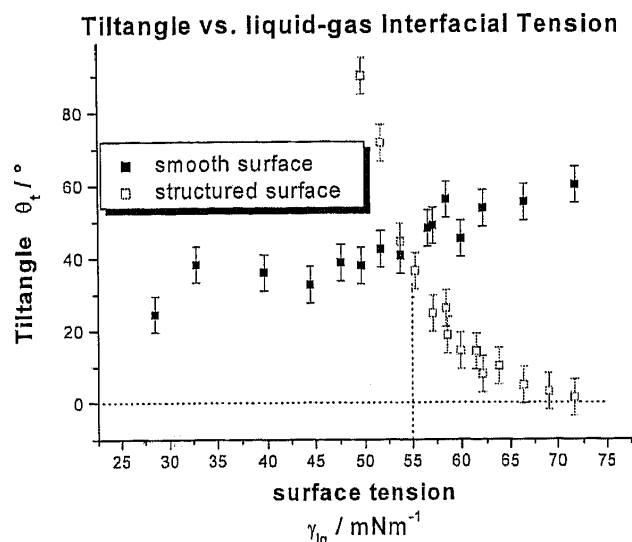


Figure 5. Tiltangle  $\theta_t$  of a smooth (filled squares) and a microstructured (open squares) surface against liquids of different surface tension.

of roughness can neither be found by a profilometric device nor by an AFM at a silica content  $>20\%$ . Therefore, hysteresis is more sensitive to morphological variations than roughness parameters and can be seen as an analytical parameter by itself.

In practice, it is useful to know whether a liquid forms droplets or runs off a structured hydrophobic surface. Of course, this is dependent on the inclination of the surface and the tiltangle  $\theta_t$  therefore allows a direct characterization of the surface in this respect. Interestingly, a drop of water may adhere at surfaces of the Wenzel-Regime even at  $\theta_t = 90^\circ$ . Therefore,  $\theta_t$  is restricted to values of  $0^\circ$ – $90^\circ$ .

We investigated  $\theta_t$  of a superhydrophobic surface against a series of liquids of various surface tensions in the range of  $30$ – $72 \text{ mN}\cdot\text{m}^{-1}$  and compared it to  $\theta_t$  of the respective smooth surface (Fig. 5).

On the smooth hydrophobic surface  $\theta_t$  increases about linearly with surface tension. In contrast, the superhydrophobic surface has a completely different behavior. On the structured surface,  $\theta_t$  decreases dramatically with increasing surface tension. At surface tensions  $\gamma_{lg} < 47 \text{ mN}\cdot\text{m}^{-1}$ ,  $\theta_t$  is undeterminable because the drop adheres to the surface even at  $\theta_t = 90^\circ$ . For water ( $\gamma_{lg} 72 \text{ mN}\cdot\text{m}^{-1}$ )  $\theta_t$  is less than  $1^\circ$ , demon-

strating the superhydrophobicity of the surface. The comparison of the two surfaces allows the definition of a critical surface tension  $\gamma_c$ , where  $\theta_t$  (smooth surface) =  $\theta_t$  (microstructured surface). The microstructured surface provides better run-off of liquids  $\gamma_{lg} > \gamma_c$ , whereas smooth surfaces are favorable for liquids  $\gamma_{lg} < \gamma_c$ . Therefore,  $\gamma_c$  allows to characterize the pattern and the applicability of a structured hydrophobic surface. For the investigated surface,  $\gamma_c \approx 55 \text{ mN}\cdot\text{m}^{-1}$ . Future studies will address a further reduction of  $\gamma_c$  to widen the scope of application of the coating.

## 1. Conclusion

The wettability of microstructured hydrophobic surfaces is investigated and discussed in terms of surface morphology. Using different kind and amount of silica nano-particles the surface morphology can be effectively controlled. The wettability can be regarded as a sensitive analytical parameter for the surface morphology. The complete range of wettability regimes is accessible as characterized by the dynamic contact angles against water. Superhydrophobic surfaces are obtained using fumed silica. By comparison of tiltangles against liquids of different surface tension a critical surface tension  $\gamma_c$  is identified, which can be taken to further characterize structure and applicability of superhydrophobic surfaces.

## References

1. H. Schmidt, in *Organosilicon Chemistry II*, edited by N. Auner and J. Weis (VCH, Weinheim, 1996), p. 737.
2. P. Müller, S. Pilotek, A. Poppe, and H. Schmidt, in *Wörlitzer Workshop* (Fördergemeinschaft Dünne Schichten, Dessau, 2000).
3. T. Onda, S. Shibuichi, N. Satoh, and K. Tsujii, *Langmuir* **12**, 2125 (1996); K. Tadanaga, N. Katata, and T. Minami, *J. Am. Ceram. Soc.* **80**, 1040 (1997); M. Miwa, A. Nakajima, A. Fujishima, K. Hashimoto, and T. Watanabe, *Langmuir* **16**, 5754 (2000); A. Nakajima, K. Hashimoto, and T. Watanabe, *Monatshefte für Chemie* **31**, 132 (2001).
4. R.E. Johnson and R.H. Dettre, in *Surface and Colloid Science*, vol. 2, edited by E. Matijevic (Wiley, New York, 1969), p. 85.
5. D. Öner and T.J. McCarthy, *Langmuir* **16**, 7777 (2000).